

The role of the DNA sensor STING in protection from lethal infection following corneal and intracerebral challenge with HSV-1.

3

4 Zachary M. Parker¹, Aisling A. Murphy^{1,2}, David A. Leib¹

5

6 Department of Microbiology and Immunology¹, Geisel School of Medicine at Dartmouth,
7 Lebanon, NH 03756

8

9 Running title: STING and HSV-1 pathogenesis

10

11 *Corresponding author:

12 David A. Leib, PhD.

13 Geisel School of Medicine at Dartmouth

14 Department of Microbiology and Immunology

15 630E Borwell Building

16 One Medical Center Drive HB 7556

17 Lebanon, NH 03756.

18

19

19 Tel: (603) 650-8616 Fax: (603) 650-6223

20 david.a.leib@dartmouth.edu

21

²² ² Current address: School of Biomedical and Healthcare Sciences, Plymouth University, UK²

23 Abstract word count: 246 words

24

STING and HSV-1 pathogenesis

25 **ABSTRACT**

26 **STING is a protein in the cytosolic DNA and cyclic dinucleotide sensor pathway that is critical for**
27 **the initiation of innate responses to infection by various pathogens. Consistent with this, HSV-1**
28 **causes invariable and rapid lethality in STING-deficient ($STING^{-/-}$) mice following intravenous (iv)**
29 **infection. In this study, using real-time bioluminescence imaging and virological assays, as**
30 **expected, we demonstrated that $STING^{-/-}$ mice support greater replication and spread in ocular**
31 **tissues and the nervous system. In contrast, they did not succumb to challenge via the corneal route**
32 **even with high titers of a virus that was routinely lethal to $STING^{-/-}$ mice by the iv route. Corneally-**
33 **infected $STING^{-/-}$ mice also showed increased periocular disease, increased corneal and trigeminal**
34 **ganglia titers although no difference in brain titers. They also showed elevated expression of TNF α**
35 **and CXCL9 relative to control mice, but surprisingly modest changes in type I interferon**
36 **expression. Finally, we also showed that HSV strains lacking the ability to counter autophagy and**
37 **the PKR-driven antiviral state had near-wild-type virulence following intracerebral infection of**
38 **$STING^{-/-}$ mice. Together, these data show that while STING is an important component of host**
39 **resistance to HSV in the cornea, its previously-shown immutable role in mediating host survival by**
40 **the iv route was not recapitulated following a mucosal infection route. Furthermore, our data are**
41 **consistent with the idea that HSV counters STING-mediated induction of the antiviral state and**
42 **autophagy response, both of which are critical factors for survival following direct infection of the**
43 **nervous system.**

44

45

46

47

48

STING and HSV-1 pathogenesis

49 **IMPORTANCE**

50 **HSV infections represent an incurable source of morbidity and mortality in humans, and are**
51 **especially severe in neonatal and immune-compromised populations. A key step in development of**
52 **an immune response is the recognition of microbial components within infected cells. The host**
53 **protein STING is important in this regard for the recognition of HSV DNA, and the subsequent**
54 **triggering of innate responses. STING was previously shown to be essential for protection against**
55 **lethal challenge from intravenous HSV-1 infection. In this study we show that the requirement for**
56 **STING depends on the infection route. In addition, STING is important for appropriate regulation**
57 **of the inflammatory response in the cornea, and our data are consistent with the idea that HSV**
58 **modulates STING activity through inhibition of autophagy. Our results elucidate the importance of**
59 **STING in host protection from HSV-1, and demonstrate the redundancy of host protective**
60 **mechanisms, especially following mucosal infection.**

61

62 **148 words**

63

64

65

66

67

68

69

70

71

STING and HSV-1 pathogenesis

72 INTRODUCTION

73 Herpes simplex virus type-1 (HSV-1) is a member of the *Alphaherpesvirus* subfamily with high
74 seroprevalence in the human population (1). Infection at mucosal surfaces such as the mouth, eyes, and
75 genitalia leads initially to lytic replication in mucosal epithelial cells, followed by infection of the
76 innervating sensory neurons. HSV-1 then travels in a retrograde direction to the neuronal cell body where
77 it establishes latency. It is this ability to establish latency that renders HSV-1 refractory to clearance by
78 the immune system, allowing persistence for the lifetime of the host. During periods of reactivation from
79 latency, HSV-1 can travel in the anterograde direction to mucosal tissues causing diseases ranging in
80 severity from the common cold sore, to herpetic stromal keratitis (HSK), the most common cause of
81 infectious blindness in the developed world (2). HSV-1 can also gain entry into the central nervous
82 system (CNS) to cause herpes simplex encephalitis (HSE) (3). HSE is a leading cause of viral
83 encephalitis, further underscoring the significant morbidity and mortality associated with HSV-1.

84 In order to effectively respond to infection, host cells have evolved a broad spectrum of sensors
85 of evolutionarily-conserved pathogen-associated molecular patterns or PAMPs (for reviews see (4, 5)).
86 To establish a directed and metered antiviral state, the cellular responses to viral nucleic acids are
87 particularly important. While responses to endosomal nucleic acids by TLR3, TLR7, and TLR9 have been
88 well-studied, our understanding of responses to cytosolic nucleic acids is less developed (4, 6). Such
89 cytoplasmic sensing pathways are candidates for efficient sensing of HSV because genomic HSV-1 DNA
90 is found free in the cytoplasm following proteosomal degradation of the HSV-1 virion (7). STING (also
91 known as MITA, ERIS, and TMEM173) is an adaptor protein activated by cytosolic dsDNA or cyclic
92 dinucleotides (8–12). Once activated, STING translocates to the endoplasmic reticulum, activating the
93 TBK1/IRF3 pathway which upregulates interferon (IFN) β (9). In addition, IFI16, a ligand of STING, is a
94 DNA sensor that presents nuclear and cytoplasmic HSV DNA to STING, thereby potentiating the
95 STING-dependent sensing of infection (13, 14)). Consistent with this, STING is critical for survival of
96 mice following high titer intravenous HSV-1 infection (15). An additional study showed that STING-

STING and HSV-1 pathogenesis

97 deficient mice have increased HSV-1 titers in corneas relative to control mice, but no further parameters
98 of pathogenesis were measured (16). These studies confirm a role for STING in HSV infection, and
99 collectively suggest that STING-deficiency renders the host highly susceptible to HSV infection,
100 equivalent perhaps to deficiencies in STAT1, type I IFN receptors, or IRF3/7 (17–20). These studies
101 notwithstanding, it remains unknown how STING-driven responses shape HSV pathogenesis following
102 peripheral challenge. The efficacy of STING-driven responses to HSV varies by cell type *in vitro*, which
103 further complicates predictions of the role of STING *in vivo* (9, 15, 21). Furthermore, recent work has
104 demonstrated crosstalk between the STING and autophagy pathways, and shown it to be important for
105 activating IRF-3 (22, 23). These host defenses notwithstanding, HSV encodes a variety of genes that
106 serve to counter IFN-driven innate responses, and autophagy (24–27). The γ 34.5 gene of HSV-1 is an
107 especially potent neurovirulence factor in mice and humans that serves to counter the IFN and PKR-
108 driven antiviral state, as well as strongly modulating the autophagy/xenophagy through a specific
109 interaction with the essential autophagy protein Beclin 1 (24, 28, 29). This provokes the idea that through
110 γ 34.5, HSV may thereby inhibit the STING-driven response through its ability to modulate the autophagy
111 pathway (30).

112 In this study we examined central (intravenous and intracerebral) and peripheral (ocular) routes of
113 HSV-1 infection in STING-deficient and control mice. In agreement with previous studies, we found
114 STING was essential for control of HSV-1 following central challenge. In contrast to previous studies,
115 however, STING was dispensable for survival following peripheral challenge even with high titers of
116 virus that were routinely lethal to STING^{-/-} mice at low intravenous doses. We also demonstrate a role for
117 TNF α and CXCL9 in the increased pathology observed in STING-deficient mice, and show that γ 34.5
118 counters both STING-driven antiviral and autophagy responses in the infected host.

119

120

121

STING and HSV-1 pathogenesis

122 **MATERIALS & METHODS**

123 **Viruses, Cells, and Mice.** Vero cells were used to propagate and titer viruses as described previously
124 (31). The wild-type HSV-1 strains used were strain KOS and strain 17 syn⁺ (32, 33). KOS/Dlux/OriL, the
125 luciferase-expressing HSV strain used for bioluminescent imaging (BLI), was previously described (34).
126 The γ 34.5-null virus ($\Delta\gamma$ 34.5), γ 34.5 beclin-binding domain-deleted virus Δ 68H (termed herein Δ BBD),
127 and thymidine kinase null virus 17/tBTK⁻ (termed herein Δ TK) were all on strain 17 syn⁺ background and
128 described previously (35–37). Heterozygous STING^{+/−} mice in a mixed C57BL/6 and 129SvEv
129 background were generously provided by Glen Barber (University of Miami) and described previously
130 (9). This study was carried out in accordance with guidelines set forth by the *Guide for the Care and Use*
131 *of Laboratory Animals* of the National Institutes of Health. Our protocols were approved by the
132 Dartmouth IACUC Committee (05/06/12, approval number leib.da.1).

133

134 **Animal Infection, Organ Harvest, Periocular Disease Scoring.** Heterozygous STING^{+/−} mice were bred
135 to generate STING^{−/−} and wild type littermate control mice and genotyped according to methods and
136 primers described previously (9, 38). Male and female mice, aged 6–14 weeks, were anesthetized with IP
137 injection of ketamine (87 mg/kg body weight) and xylazine (13 mg/kg body weight). Corneas were
138 scarified in a 10 × 10 crosshatch pattern and mice were either inoculated with 2×10^6 pfu virus (unless
139 otherwise noted) in 5 μ L of inoculation medium [Dulbecco's Modified Eagle's Medium (DMEM)
140 (HyClone) with 2% fetal bovine serum, penicillin at 60 units/mL (HyClone), and streptomycin at 60
141 μ g/mL (HyClone) final concentration], or mock infected with 5 μ L of innoculum medium (31). For
142 intracranial infections, mice were anesthetized as described above, and then injected with 1×10^4 pfu of the
143 indicated virus in 10 μ L inoculum medium using a Hamilton syringe and a 26G needle. For intravenous
144 infections 1×10^7 pfu of strain KOS in a volume of 150 μ L was injected directly into tail veins.

145 Mice were sacrificed at the specified times postinfection or once they met endpoint criteria as
146 defined by our IACUC protocol. Eye swabs were collected at indicated time points as previously

STING and HSV-1 pathogenesis

147 described (39). Blood was harvested and serum was separated by centrifugation at 2000rcf for 5 minutes
148 and then stored at -80°C. Eye swabs, spleens, livers, brains, brain stems, and trigeminal ganglia were
149 frozen in the appropriate volume of inoculation medium at -80°C. Tissues were prepared for titering by
150 homogenization/disruption with glass beads and sonication as previously described (31).

151 Mice were scored for disease and weighed at the specified times postinfection. Periocular disease
152 scoring was performed as previously described and summarized here: 0- no pathology, 0.5- minor eyelid
153 swelling, 1.0- minor eyelid and nasal swelling, 1.5- moderate eyelid and nasal swelling, 2.0- severe eyelid
154 swelling with minor periocular hair loss and skin damage, 3.0- neurological symptoms (20).

155

156 **IFN β Enzyme-Linked Immunosorbent Assay (ELISA).** Mice were infected as indicated previously
157 and organs were harvested, weighed, and placed in extraction reagent I (Invitrogen, CA). Organs were
158 homogenized using an electric (Omni International, GA) homogenizer prior to ELISA. Samples were then
159 centrifuged and supernatants analyzed using an IFN- β ELISA-HS kit according to manufacturer's
160 instructions (PBL Interferon Source, NJ).

161

162 **Quantitative Real-Time PCR.** Organs were harvested into tissue extraction reagent I (Invitrogen, CA)
163 and then homogenized (Omni International, GA) at the timepoints indicated. RNA was extracted using
164 Trizol (Life Technologies, NY), and further purified using an RNeasy kit (Qiagen). cDNA was
165 synthesized using SuperScript III (Life Technologies, NY) and random hexamer primers (Promega, WI).
166 This cDNA was used for SYBR Green real-time PCR (Life Technologies, NY). IFIT1 and TNF α were
167 measured relative to GAPDH using primers as previously described (40, 41) and analyzed using the 2 $^{-\Delta\Delta CT}$
168 method (42).

169

170 **Cytokine Quantification.** Organs were harvested into tissue extraction reagent (Invitrogen, CA) and
171 homogenized (Omni International, GA) at the timepoints indicated. Cytokines were quantified using a
172 mouse 32plex Luminex assay (MPXMCYTO70KPMX32, EMD Millipore, Germany). CXCL9 levels

STING and HSV-1 pathogenesis

173 were further analyzed using the bead-based cytokine quantification assay Super X-Plex (Antigenix
174 America, NY) according to manufacturer's instructions with samples treated as per the Luminex assay.

175

176 **Bioluminescent Imaging (BLI).** Mice infected corneally with KOS/Dlux/OriL and at the appropriate
177 times postinfection were injected IP with filter-sterilized D-luciferin potassium salt (Gold Biotech, MO)
178 in PBS at 150 μ g/g body weight. Mice were anesthetized with 2.5% isoflurane and imaged using a cooled
179 charge-coupled device (CCD) camera equipped instrument (IVIS 100, Caliper LifeSciences, MA) as
180 previously described (43). Mice were imaged for 30 seconds, f-stop 1, binning 8, and a field of view of
181 6.6. To quantify luminescent signals, identical regions of interest (ROI) were placed over images
182 encompassing the mouse's head from the dorsal view. ROI results were recorded using total photon flux
183 in photons/second per ROI. All images were analyzed using Igor Pro Living Image Software (Version
184 2.60) (PerkinElmer, OH).

185

186

187

188

189

190

191

192

193

194

195

STING and HSV-1 pathogenesis

196 **RESULTS**

197 **STING is dispensable for protection from lethality following peripheral HSV-1 infection.**

198 We wished to address the hypothesis that the impact of STING on HSV pathogenesis is
199 dependent on the route of infection. Previous results demonstrated that infection of STING^{-/-} mice was
200 uniformly lethal following iv infection with 1×10^7 pfu HSV-1 strain KOS, while $\geq 75\%$ control mice
201 survived (15). We wanted to determine whether this mortality pattern would occur following infection at
202 peripheral sites such as the cornea, a natural route of infection in humans. To match the lethal input
203 inoculum of the previously published iv study we used 1×10^7 pfu KOS. This dose is significantly higher
204 than that required for IFN $\alpha\beta\gamma$ R^{-/-}, STAT1^{-/-} or IRF-7^{-/-} mice to succumb to corneal infection (20, 44). We
205 therefore infected STING^{-/-} and littermate control mice either via the cornea, the tail vein (iv), or the
206 cerebrum (ic) with HSV-1 KOS and observed the mice for 21 days or until endpoint health criteria were
207 reached (Fig. 1A-C). Surprisingly, STING^{-/-} and control mice corneally infected with 1×10^7 pfu KOS were
208 comparable in terms of survival, with 1/9 of STING^{-/-} mice and 0/11 control mice reaching endpoint
209 criteria within 21 days (Fig. 1A). In contrast, following iv infection with 1×10^7 pfu KOS, 7/8 STING^{-/-}
210 mice reached endpoint criteria within 7 days relative to only 3/10 control mice (Fig. 1B). To assess
211 whether STING plays an important role during infection within tissues of the CNS, mice were infected ic
212 with 1×10^4 pfu HSV-1 KOS. We observed that 13/14 ic infected STING^{-/-} mice reached endpoint criteria
213 within 5 days postinfection (Fig. 1C), in stark contrast to only 1/14 control mice reaching endpoint
214 criteria within the 21-day experimental period. Consistent with this increased mortality following ic
215 infection, we also observed significantly increased viral titers in the brains of STING^{-/-} relative to control
216 mice when infected ic (Fig. 1D). Taken together, these data confirm the requirement for STING in
217 protecting the host from HSV-1 in the CNS. In addition, reduced mortality following peripheral challenge
218 suggests a STING-independent bottleneck to lethal infection via the cornea when infected with HSV-1
219 strain KOS.

220

STING and HSV-1 pathogenesis

221 **STING protects the cornea from acute HSV infection but is not required for viral clearance.**

222 To gain a rapid overview of viral replication and spread we used real-time bioluminescent
223 imaging (BLI) in conjunction with KOS/Dlux/OriL (KOSDLux), a virus which expresses firefly luciferase
224 (32, 34). Following corneal infection with 2×10^6 pfu/eye of KOSDLux, STING^{-/-} and control mice were
225 imaged daily on days 2 through 9 postinfection (dpi). Significant luciferase activity above baseline was
226 observed in the eyes and the skin of the snout of both strains of mice on days 4 through 7 (Fig. 2A and
227 data not shown). Quantification of the BLI signals revealed a significantly higher photon flux in the
228 STING^{-/-} mice relative to littermate controls over the 9-day timecourse (Fig. 2B). Despite this increase,
229 photon flux in both the STING^{-/-} and wild type mice returned to baseline on day 9, indicating both strains
230 of mice were able to clear the infection in the cornea (Fig. 2B). Consistent with this, the visceral
231 dissemination and mortality previously observed with corneal KOSDLux infection of IFN $\alpha\beta\gamma$ R^{-/-} and
232 STAT1^{-/-} mice was not observed in STING^{-/-} mice (44). These results demonstrate that while STING
233 plays a role in the control of corneal HSV-1 infection, it is dispensable for the clearance of virus from the
234 cornea and from tissues subsequently infected via this route.

235 To confirm and extend our BLI results to tissues that cannot be easily imaged, STING^{-/-} mice and
236 littermate controls were corneally infected with 2×10^6 pfu/eye of HSV-1 KOS and viral titers were
237 quantified in corneas, brain, brain stem, liver, spleen, lymph nodes, and serum. STING^{-/-} mice had
238 significantly increased viral titers compared to control mice in both eyes and trigeminal ganglia (Fig.
239 3A,B). Viral loads within the brain stem (Fig. 3C) and brain tissues (Fig. 3D) did not significantly differ
240 between control and STING^{-/-} mice, confirming that there is no additional dissemination through the
241 tissues of the CNS following peripheral infection. This was in contrast to mice that were infected ic, in
242 which there were significantly increased titers in the brains of STING^{-/-} mice (Fig. 1D). Virus was not
243 detected in the serum, lymph nodes, spleens, or livers of STING^{-/-} or control mice on days 3 and 5
244 postinfection (data not shown), confirming lack of visceral dissemination following peripheral challenge.

245 Given the increased titers in corneas and trigeminal ganglia of STING^{-/-} mice we wished to assess
246 whether these mice would also exhibit altered periocular disease or weight loss (Fig. 3E, F). Periocular

STING and HSV-1 pathogenesis

247 disease scores were significantly higher for STING^{-/-} than control mice on 6 of 10 days monitored
248 postinfection, and at all time points the mean disease scores were higher for the STING^{-/-} mice. The
249 weight loss of STING^{-/-} mice was overall greater than control mice although it failed to reach statistical
250 significance except for 8 days postinfection. Taken together, these data suggest that there is STING-
251 dependent control of viral replication in the cornea, but that STING is dispensable for viral clearance.
252 Moreover, STING-deficiency is associated with significantly increased periocular disease.

253

254 **Interferon responses of STING^{-/-} mice following corneal infection.**

255 STING acts as an adaptor which bridges cytosolic DNA sensing with upregulation of IFN β – a
256 critical cytokine in host defense to viral infection (45–47). We observed in this study that the survival of
257 STING^{-/-} mice was dependent upon the route of infection. We therefore hypothesized that the survival
258 differences observed in STING^{-/-} mice might result from anatomically distinct patterns of IFN β signaling.
259 To test this hypothesis, we ocularly infected STING^{-/-} and control mice with HSV-1 KOS and measured
260 IFN β in the cornea by ELISA (Fig. 4A). At 3 days post corneal infection IFN β levels were significantly
261 elevated in infected, relative to mock-infected corneas. Surprisingly, IFN β levels were slightly higher in
262 the STING^{-/-} corneas relative to littermate controls (Fig. 4A). We also measured IFN β levels in brain
263 tissue of mice following intracranial infection with HSV-1 KOS. Again, at 3 days post ic infection IFN β
264 levels were significantly elevated in infected, relative to mock-infected brains (Fig. 4B). Consistent with
265 previous studies, slightly lower levels of IFN β were observed in STING^{-/-} mice compared to littermate
266 controls (15). To further measure IFN synthesis following corneal and ic infections at earlier time points,
267 we also measured IFN at 2,4,6, and 8 hours postinfection, but all samples were at or below the level of
268 detection of the ELISA (data not shown).

269 Although these differences in IFN β levels in the corneas and brains of STING^{-/-} relative to control
270 mice were statistically significant ($p < 0.05$), the magnitude of these changes seemed insufficient to explain
271 the differences in viral pathogenesis observed. Nonetheless, it was possible that small changes in IFN β
272 levels could have a disproportionate effect on downstream anti-viral IFN stimulated genes (ISGs).

STING and HSV-1 pathogenesis

273 Furthermore, the sensitivity of ELISA for detecting IFN β could be limiting since the values obtained were
274 close to the limits of detection. To examine this further, induction of the ISG *IFIT1* was measured using
275 real-time PCR. Consistent with the patterns seen with IFN β , there was strong induction of *IFIT1*
276 expression in corneas and brains of all infected, both STING $^{-/-}$ and WT, relative to mock-infected mice
277 (Fig. 4C,D). Furthermore, levels of *IFIT1* expression were statistically indistinguishable in STING $^{-/-}$ and
278 control mice. Together, these data are consistent with the idea that the increased pathology and lethality
279 caused by HSV infection in STING $^{-/-}$ relative to control mice are largely independent of the expression
280 and downstream effects of IFN β .

281

282 **Other cytokine responses in STING $^{-/-}$ mice.**

283 Given that the different survival phenotypes arising in STING $^{-/-}$ and control mice following
284 central or peripheral HSV-1 infection appeared to be independent of IFN synthesis, we hypothesized that
285 a dysregulated immune response may be causing the pathology observed. A key early regulator that
286 mediates corneal damage during HSV-1 infection is tumor necrosis factor α (TNF α) (48, 49). Using real-
287 time PCR we measured TNF α expression in corneas dissected from STING $^{-/-}$ and control mice infected
288 with HSV-1 KOS on day 3 postinfection (Fig. 5A). TNF α expression was significantly elevated in
289 corneas of STING $^{-/-}$ mice relative to control or mock-infected mice. Following ic infection, however,
290 TNF α expression was comparable in STING $^{-/-}$ and control mice (Fig. 5B). To further probe potential
291 chemokines and cytokines that may contribute to the outcomes of corneal and ic infection of STING $^{-/-}$ and
292 control mice we performed a 32-plex Luminex screen (data not shown). The corneas of corneally infected
293 STING $^{-/-}$ mice showed a particularly strong increase in the chemokine CXCL9 (Fig. 5C), consistent with
294 the observation that that infected STING $^{-/-}$ corneas exhibit increased inflammation. In contrast, wild type
295 and STING $^{-/-}$ mice infected ic showed comparable brain CXCL9 expression, although both groups had
296 elevated CXCL9 compared to mock-infected mice (Fig. 5D). Corneas of STING $^{-/-}$ mice therefore exhibit

STING and HSV-1 pathogenesis

297 elevated inflammatory cytokine responses to HSV-1 infection. In contrast, there were no demonstrable
298 differences in inflammatory cytokines between STING^{-/-} and control mice following ic infection.

299 **Virulence of γ 34.5-deficient viruses is restored in STING^{-/-} mice following ic infection.**

300 The STING-driven antiviral response in infected cells activates, and is modulated by, autophagy
301 (22, 23, 30, 50). Given the autophagy-modulating role of HSV-1 γ 34.5, it was of interest to examine its
302 role in modulating the effects of STING (24). We used two different recombinant viruses (Δ 34.5 and
303 Δ BBD) with mutations in the γ 34.5 gene. Δ 34.5 lacks the entire γ 34.5 ORF, and is thereby unable to
304 block the IFN and PKR-driven antiviral response, and cannot counter autophagy (35, 36, 51). Δ BBD is
305 fully capable of blocking the IFN and PKR-driven antiviral response, but cannot block autophagy because
306 the beclin-binding domain of γ 34.5 has been deleted (34). As a control, we also used 17 Δ TK (17/tBTK⁻)
307 which lacks the viral thymidine kinase gene (37). 17 Δ TK is highly attenuated *in vivo* through a pathway
308 unrelated to IFN responses or autophagy, and therefore served to test the caveat that STING-deficiency
309 may non-specifically increase or restore the virulence of any attenuated virus. All viruses used in these
310 experiments were in the strain 17 background. While strain 17 has higher virulence than KOS, the mutant
311 viruses are profoundly attenuated. To increase the probability of determining a clear phenotype with these
312 strain 17 mutants we therefore used a higher inoculum (2×10^4 pfu) in these ic experiments than in those
313 with KOS shown in Figs. 1C and 1D. For consistency within this experiment we also used this higher
314 inoculum with wt strain 17 (Fig. 6).. Control mice showed a significant ($p < 0.02$) survival advantage
315 compared to STING^{-/-} mice, although all mice reached endpoint criteria by 6 days postinfection (Fig. 6A).
316 When lower doses of strain 17 (50 pfu) were administered, 82% of STING^{-/-} and 91% of control mice
317 succumbed to infection, although a significant survival advantage for control mice was again observed
318 ($p < 0.02$, data not shown), consistent with the data for KOS (Fig. 1C). To test whether STING-dependent
319 antiviral responses against HSV were dependent on autophagy and whether HSV can counter this
320 response, we infected STING^{-/-} and control mice ic with Δ BBD (Fig. 6B). As previously shown, Δ BBD
321 was significantly attenuated in control animals relative to strain 17 with only 50% of mice reaching

STING and HSV-1 pathogenesis

322 endpoint criteria within 21 days (28). In contrast, in STING^{-/-} mice the virulence of ΔBBD was
323 significantly increased compared to littermate controls, with all STING^{-/-} mice succumbing to infection
324 within 8 days. We next infected with the γ34.5 null mutant (Δγ34.5) which cannot modulate autophagy,
325 and is unable to dephosphorylate eIF2α to prevent host-imposed translational arrest (29, 52). Upon
326 infection of control mice with Δγ34.5 there was profound attenuation with all control mice surviving
327 infection to 21 days (Fig. 6C). In contrast, all STING^{-/-} mice succumbed to infection with Δγ34.5 within 9
328 days (Fig. 6C), with kinetics that were statistically indistinguishable from those following infection with
329 ΔBBD (Fig. 6B). To confirm that these changes in virulence in STING^{-/-} mice were specific to the IFN
330 and autophagy pathways, we infected STING^{-/-} mice and controls with ΔTK (Fig. 6D). We observed
331 complete survival of both wild type and STING^{-/-} mice over the 21-day infection period, supporting the
332 idea that the attenuation of the γ34.5 mutants is largely due to their inability to counteract the STING-
333 dependent autophagy pathway.

334 To further understand the role of STING in corneal infection, STING^{-/-} and littermate control
335 mice were infected corneally with strain 17, Δγ34.5, ΔBBD and ΔTK virus. The inoculum used for all
336 experiments was 1x10⁵ pfu/eye, as strain 17 is more neurovirulent than strain KOS. Following HSV-1
337 strain 17 corneal infection, all STING^{-/-} mice, and 57% of control mice succumbed to infection (Fig. 7A).
338 To test whether HSV-1 counters this STING-dependent autophagic response through the BBD domain of
339 γ34.5, we infected mice corneally with ΔBBD (Fig. 7B). All STING^{-/-} mice succumbed to this infection
340 by day 11 post infection, while all control mice survived the challenge. The comparable endpoint of
341 STING^{-/-} mice infected with strain 17 and ΔBBD, along with the increased survival of control mice,
342 demonstrates that the HSV-1 γ34.5 BBD is most likely countering the STING-dependent autophagy
343 response following corneal infection. STING^{-/-} and control mice infected with Δγ34.5 showed no
344 statistically significant difference in survival (Fig. 7C). To confirm these results were specific to the
345 autophagy and IFN pathways, we corneally infected STING^{-/-} and control mice with ΔTK (Fig. 7D). We
346 found that all mice survived the ΔTK corneal challenge. Together with Figure 1, these data suggest that

STING and HSV-1 pathogenesis

347 neurovirulent strains of HSV-1 can overcome the corneal STING-independent barrier to cause significant
348 mortality, and protection is mediated at least partially by STING.

349 **DISCUSSION**

350 STING is pivotal in the innate response to a variety of pathogens (15, 50, 53, 54). This is largely
351 through its ability to recognize cytosolic dsDNA and subsequently interact with TBK, facilitating
352 phosphorylation of IRF-3 and induction of IFN-dependent antiviral responses. Consistent with these
353 activities, STING is indispensable for the protection of mice from HSV-1 induced mortality following
354 intravenous challenge with the low virulence HSV-1 KOS strain (15). The studies described herein are
355 consistent with these findings, but our use of a mucosal route of infection via the cornea has revealed that
356 STING is dispensable for survival following a peripheral challenge with KOS. These findings contrast
357 with studies of other mediators of the IFN response, such as STAT1 and IFN receptors, which are
358 essential for prevention of generalized infection and mortality following peripheral challenge with KOS.
359 Our findings also provide an interesting contrast with mice deficient in IRF-3 which were originally
360 shown to be completely resistant to challenge by intravenous HSV-1, but subsequently shown to be
361 susceptible to lethal infection via the corneal and ic routes (55, 56). These data therefore underscore the
362 importance of testing immune-deficient mice using a variety of infection routes. Furthermore, they show
363 that even when the immune deficiencies are in the same antiviral pathways, different and unexpected
364 resistance patterns can emerge.

365 IFN responses are a key determinant of the outcome of corneal infection by HSV-1. In this study
366 STING^{-/-} mice exhibited increased ocular titers relative to controls, consistent with previous studies (16).
367 Using IVIS imaging we were able to extend these observations and visualize viral tropism over a longer
368 timecourse, allowing us to observe a more robust ocular infection in STING^{-/-} mice but with eventual
369 clearance of the virus. This pattern was predicted based on previous studies but it was unexpected that the
370 altered titers were largely independent of IFN production in the tissues examined. One possible
371 explanation is that the STING pathway induces autophagy, which in turn controls virus replication in the

STING and HSV-1 pathogenesis

372 cornea (22, 23). STING^{-/-} mice may therefore have reduced ability to control HSV through
373 autophagy/xenophagy in the cornea, and as discussed further below, this may also apply to infection of
374 CNS tissues. It was also notable that STING^{-/-} mice had greater periocular disease scores compared to
375 control mice. This was consistent with increased *TNFα* expression and CXCL9 concentration in the
376 corneas of STING^{-/-} mice. Given that STING up-regulates the expression of *TNFα*, it seems likely that the
377 increased *TNFα* expression in STING^{-/-} mice results indirectly from increased viral titers, rather than a
378 direct consequence of STING-deficiency (57). Histology performed on corneas of infected mice revealed
379 increased immune cell infiltration in the corneas of STING^{-/-} mice when compared to controls (data not
380 shown), consistent with the increases in observed *TNFα* and CXCL9. While STING is clearly dispensable
381 for mediating survival following corneal infection with strain KOS, it is important for limiting HSV
382 replication in the cornea and thereby necessary to avoid the induction of immunopathological cytokine
383 expression, and subsequent periocular disease. These findings are consistent with previous data showing
384 increased and protracted genital inflammation in STING^{-/-} mice following vaginal infection, although no
385 survival data were presented (15). Furthermore, it has been observed during skin infections with HSV-1
386 that while STING^{-/-} mice have higher viral titers in the skin, virus is not found in the brain and STING^{-/-}
387 mice do not succumb to infection (Bedoui, personal communication).

388 The patterns of HSV replication and virulence in the brains of STING^{-/-} mice in this study appear
389 to be determined largely by the route of infection. Following corneal infection with HSV-1 KOS, despite
390 significantly increased titers in the cornea and trigeminal ganglia of STING^{-/-} mice, there is no difference
391 in viral replication in the brain, or statistically discernible changes in survival. Furthermore, analysis of
392 brain cytokines by BioPlex and ELISA on days 3 and 5 post corneal infection showed no significant
393 changes (data not shown). In contrast, following ic infection of STING^{-/-} mice with HSV-1 KOS we
394 observed significant changes in viral replication in the brain, pro-inflammatory cytokine production, and
395 survival. Both ic infections with KOS and 17 demonstrated a significant survival advantage for control
396 over STING^{-/-} mice. This survival advantage is greater for KOS, as expected given its reduced

STING and HSV-1 pathogenesis

397 neurovirulence relative to strain 17, but both survival phenotypes are representative of importance of
398 STING when natural barriers to infection are breached. When the neurovirulent strain 17 was used in
399 corneal infections, >50% of control mice, and 100% STING^{-/-} mice succumbed to the infection,
400 demonstrating that neurovirulence of the virus can overcome the corneal replication bottleneck. It is
401 possible that once the more neurovirulent virus is able to reach the brain, a STING-dependent response is
402 necessary to control the virus, therefore STING^{-/-} mice readily succumb to infection, although with the
403 high neurovirulence of strain 17 even half of control mice succumb to infection. These data suggest a
404 CNS-specific requirement for STING to promote host survival. The requirement for STING in the CNS,
405 however, appeared largely independent of IFN since there were only modest changes in IFN β and no
406 differences in ISG (*IFIT1*) expression between STING^{-/-} and control mice after ic infection with KOS.
407 These findings are consistent with the data and hypothesis that the nervous system largely utilizes non-
408 destructive innate responses to infection, such as autophagy/xenophagy(58, 59). This mode of pathogen
409 clearance preserves the viability of neurons which are largely a non-replicating irreplaceable population
410 of cells. IFN-driven antiviral responses are therefore necessarily muted or ineffective in the nervous
411 system, and xenophagy is a dominant antiviral defense in both the PNS and CNS. It is also of note that
412 there were no discernible differences in the ability of HSV-1 to reactivate from latently infected
413 trigeminal ganglia explanted from STING^{-/-} or control mice (data not shown). The relationship between
414 STING and autophagy is complex, and an area of a great deal of recent research. There is clear evidence,
415 however, that in addition to stimulating the IFN-driven antiviral response, STING-dependent responses
416 also stimulates the xenophagy pathway that promotes the clearance of intracellular pathogens (60).
417 Indeed, STING is critical for the HSV-induced autophagy response, at least in BMDCs (61). Notably,
418 STING transcription is low in cornea and brain tissues but high in antigen presenting cells, cells that
419 undergo significant autophagic flux (62, 63). The data described herein strongly implicate that HSV γ 34.5
420 counters the antiviral effects of STING largely through its ability to modulate autophagy through binding
421 to Beclin 1, rather than altering IFN responses through its ability to bind TBK, eIF2 α or PP1 α (22, 24, 28,

STING and HSV-1 pathogenesis

422 29, 52, 64). Further support for this idea comes from studies in our laboratory showing that IRF3
423 phosphorylation, largely mediated by TBK, is comparable between ΔBBB and wild type viruses
424 (Manivanh and Leib, Unpublished data). Data from this study are consistent with the idea that while the
425 STING-driven IFN-dependent response is important *in vivo* in some instances, the STING-dependent
426 activation in autophagy and xenophagy is also a critical antiviral mechanism, especially in the CNS. Both
427 of these responses are powerfully countered by γ34.5, and likely by other viral factors such as ICP0 and
428 US11, which act in concert to regulate the intricate lifecycle of HSV-1 (26, 27, 65).

429

430

431

432

433

434

435

436

437

438

439

440 **ACKNOWLEDGEMENTS**

441 This study was supported by National Institutes of Health grant to D.L. (RO1 EY09083). The
442 project was also supported by P30RR016437 from the National Center for Research Resources
443 to Dartmouth. Training Grant support from the Geisel School of Medicine Microbiology and
444 Molecular Pathogenesis Program Training Grant (5T32AI007519 Host-Microbe Interactions) to

STING and HSV-1 pathogenesis

445 Z.P. We also acknowledge Brian North for colony maintenance and genotyping, and Glen Barber
446 for the STING^{-/-} mice.

447 REFERENCES

- 448 1. Xu F, Sternberg MR, Kottiri BJ, McQuillan GM, Lee FK, Nahmias AJ, Berman SM,
449 Markowitz LE. August 23. Trends in Herpes Simplex Virus Type 1 and Type 2 Seroprevalence in
450 the United States. *JAMA: The Journal of the American Medical Association* **296**:964–973.
- 451 2. Rowe AM, St. Leger AJ, Jeon S, Dhaliwal DK, Knickelbein JE, Hendricks RL. 2013. Herpes
452 keratitis. *Progress in Retinal and Eye Research* **32**:88–101.
- 453 3. Kennedy PGE. 2005. Viral encephalitis. *J Neurol* **252**:268–272.
- 454 4. Arpaia N, Barton GM. 2011. Toll-like receptors: key players in antiviral immunity. *Current Opinion*
455 in Virology
- 456 5. Luecke S, Paludan SR. 2015. Innate recognition of alphaherpesvirus DNA. *Adv Virus Res* **92**:63–
457 100.
- 458 6. Barber GN. 2011. Cytoplasmic DNA innate immune pathways. *Immunological Reviews* **243**:99–
459 108.
- 460 7. Horan KA, Hansen K, Jakobsen MR, Holm CK, Søby S, Unterholzner L, Thompson M, West
461 JA, Iversen MB, Rasmussen SB, Ellermann-Eriksen S, Kurt-Jones E, Landolfo S, Damania B,
462 Melchjorsen J, Bowie AG, Fitzgerald KA, Paludan SR. 2013. Proteasomal Degradation of
463 Herpes Simplex Virus Capsids in Macrophages Releases DNA to the Cytosol for Recognition by
464 DNA Sensors. *J Immunol* **190**:2311–2319.
- 465 8. Jin L, Waterman PM, Jonscher KR, Short CM, Reisdorph NA, Cambier JC. 2008. MPYS, a
466 novel membrane tetraspanner, is associated with major histocompatibility complex class II and
467 mediates transduction of apoptotic signals. *Mol Cell Biol* **28**:5014–5026.
- 468 9. Ishikawa H, Barber GN. 2008. STING is an endoplasmic reticulum adaptor that facilitates innate
469 immune signalling. *Nature* **455**:674–678.
- 470 10. Zhong B, Yang Y, Li S, Wang Y-Y, Li Y, Diao F, Lei C, He X, Zhang L, Tien P, Shu H-B. 2008.
471 The Adaptor Protein MITA Links Virus-Sensing Receptors to IRF3 Transcription Factor
472 Activation. *Immunity* **29**:538–550.
- 473 11. Sun W, Li Y, Chen L, Chen H, You F, Zhou X, Zhou Y, Zhai Z, Chen D, Jiang Z. 2009. ERIS,
474 an endoplasmic reticulum IFN stimulator, activates innate immune signaling through dimerization.
475 *PNAS* **106**:8653–8658.
- 476 12. Burdette DL, Monroe KM, Sotelo-Troha K, Iwig JS, Eckert B, Hyodo M, Hayakawa Y, Vance
477 RE. 2011. STING is a direct innate immune sensor of cyclic di-GMP. *Nature* **478**:515–518.
- 478 13. Unterholzner L, Keating SE, Baran M, Horan KA, Jensen SB, Sharma S, Sirois CM, Jin T,
479 Latz E, Xiao TS, Fitzgerald KA, Paludan SR, Bowie AG. 2010. IFI16 is an innate immune
480 sensor for intracellular DNA. *Nat Immunol* **11**:997–1004.
- 481 14. Li T, Diner BA, Chen J, Cristea IM. 2012. Acetylation modulates cellular distribution and DNA
482 sensing ability of interferon-inducible protein IFI16. *PNAS* **109**:10558–10563.
- 483 15. Ishikawa H, Ma Z, Barber GN. 2009. STING regulates intracellular DNA-mediated, type I
484 interferon-dependent innate immunity. *Nature* **461**:788–792.
- 485 16. Conrady CD, Zheng M, Fitzgerald KA, Liu C, Carr DJJ. 2012. Resistance to HSV-1 infection in
486 the epithelium resides with the novel innate sensor, IFI-16. *Mucosal Immunology* **5**:173–183.
- 487 17. Pasieka TJ, Baas T, Carter VS, Proll SC, Katze MG, Leib DA. 2006. Functional Genomic
488 Analysis of Herpes Simplex Virus Type 1 Counteraction of the Host Innate Response. *J Virol*
489 **80**:7600–7612.

STING and HSV-1 pathogenesis

- 490 18. **Pasieka TJ, Cilloniz C, Lu B, Teal TH, Proll SC, Katze MG, Leib DA.** 2009. Host Responses to
491 Wild-Type and Attenuated Herpes Simplex Virus Infection in the Absence of Stat1. *J Virol* **83**:2075–2087.
- 492 19. **Pasieka TJ, Menachery VD, Rosato PC, Leib DA.** 2012. Corneal replication is an interferon
493 response-independent bottleneck for virulence of herpes simplex virus 1 in the absence of virion
494 host shutoff. *J Virol* **86**:7692–7695.
- 495 20. **Murphy AA, Rosato PC, Parker ZM, Khalenkov A, Leib DA.** 2013. Synergistic control of herpes
496 simplex virus pathogenesis by IRF-3, and IRF-7 revealed through non-invasive bioluminescence
497 imaging. *Virology*.
- 498 21. **Rosato PC, Leib DA.** 2014. Intrinsic Innate Immunity Fails To Control Herpes Simplex Virus and
499 Vesicular Stomatitis Virus Replication in Sensory Neurons and Fibroblasts. *J Virol* **88**:9991–10001.
- 500 22. **Liang Q, Seo GJ, Choi YJ, Kwak M-J, Ge J, Rodgers MA, Shi M, Leslie BJ, Hopfner K-P, Ha
501 T, Oh B-H, Jung JU.** 2014. Crosstalk between the cGAS DNA Sensor and Beclin-1 Autophagy
502 Protein Shapes Innate Antimicrobial Immune Responses. *Cell Host & Microbe* **15**:228–238.
- 503 23. **Konno H, Konno K, Barber GN.** 2013. Cyclic Dinucleotides Trigger ULK1 (ATG1)
504 Phosphorylation of STING to Prevent Sustained Innate Immune Signaling. *Cell* **155**:688–698.
- 505 24. **Orvedahl A, Alexander D, Tallóczy Z, Sun Q, Wei Y, Zhang W, Burns D, Leib DA, Levine B.**
506 2007. HSV-1 ICP34.5 Confers Neurovirulence by Targeting the Beclin 1 Autophagy Protein. *Cell
507 Host & Microbe* **1**:23–35.
- 508 25. **Lanfranca MP, Mostafa HH, Davido DJ.** 2014. HSV-1 ICP0: An E3 Ubiquitin Ligase That
509 Counteracts Host Intrinsic and Innate Immunity. *Cells* **3**:438–454.
- 510 26. **Ishioka K, Ikuta K, Sato Y, Kaneko H, Sorimachi K, Fukushima E, Saijo M, Suzutani T.** 2013.
511 Herpes simplex virus type 1 virion-derived US11 inhibits type 1 interferon-induced protein kinase R
512 phosphorylation. *Microbiol Immunol* **57**:426–436.
- 513 27. **Lussignol M, Queval C, Bernet-Camard M-F, Cotte-Laffitte J, Beau I, Codogno P, Esclatine A.**
514 2013. The Herpes Simplex Virus 1 Us11 Protein Inhibits Autophagy through Its Interaction with the
515 Protein Kinase PKR. *J Virol* **87**:859–871.
- 516 28. **Leib DA, Alexander DE, Cox D, Yin J, Ferguson TA.** 2009. Interaction of ICP34.5 with Beclin 1
517 Modulates Herpes Simplex Virus Type 1 Pathogenesis through Control of CD4+ T-Cell Responses.
518 *J Virol* **83**:12164–12171.
- 519 29. **Li Y, Zhang C, Chen X, Yu J, Wang Y, Yang Y, Du M, Jin H, Ma Y, He B, Cao Y.** 2011.
520 ICP34.5 protein of herpes simplex virus facilitates the initiation of protein translation by bridging
521 eukaryotic initiation factor 2alpha (eIF2alpha) and protein phosphatase 1. *J Biol Chem* **286**:24785–
522 24792.
- 523 30. **Saitoh T, Fujita N, Hayashi T, Takahara K, Satoh T, Lee H, Matsunaga K, Kageyama S,
524 Omori H, Noda T, Yamamoto N, Kawai T, Ishii K, Takeuchi O, Yoshimori T, Akira S.** 2009.
525 Atg9a controls dsDNA-driven dynamic translocation of STING and the innate immune response.
526 *Proc Natl Acad Sci U S A* **106**:20842–20846.
- 527 31. **Rader KA, Ackland-Berglund CE, Miller JK, Pepose JS, Leib DA.** 1993. In Vivo
528 Characterization of Site-Directed Mutations in the Promoter of the Herpes Simplex Virus Type 1
529 Latency-Associated Transcripts. *J Gen Virol* **74**:1859–1869.
- 530 32. **SMITH KO.** 1964. RELATIONSHIP BETWEEN THE ENVELOPE AND THE INFECTIVITY OF
531 HERPES SIMPLEX VIRUS. *Proc Soc Exp Biol Med* **115**:814–816.
- 532 33. **Brown SM, Ritchie DA, Subak-Sharpe JH.** 1973. Genetic studies with herpes simplex virus type 1.
533 The isolation of temperature-sensitive mutants, their arrangement into complementation groups and
534 recombination analysis leading to a linkage map. *J Gen Virol* **18**:329–346.
- 535 34. **Summers BC, Leib DA.** 2002. Herpes Simplex Virus Type 1 Origins of DNA Replication Play No
536 Role in the Regulation of Flanking Promoters. *J Virol* **76**:7020–7029.
- 537 35. **English L, Chemali M, Duron J, Rondeau C, Laplante A, Gingras D, Alexander D, Leib D,
538 Norbury C, Lippé R, Desjardins M.** 2009. Autophagy enhances the presentation of endogenous
539 viral antigens on MHC class I molecules during HSV-1 infection. *Nat Immunol* **10**:480–487.
- 540

STING and HSV-1 pathogenesis

- 541 36. **Alexander DE, Ward SL, Mizushima N, Levine B, Leib DA.** 2007. Analysis of the Role of
542 Autophagy in Replication of Herpes Simplex Virus in Cell Culture. *J Virol* **81**:12128–12134.
543 37. **Thompson RL, Sawtell NM.** 2000. Replication of Herpes Simplex Virus Type 1 within Trigeminal
544 Ganglia Is Required for High Frequency but Not High Viral Genome Copy Number Latency. *J
545 Virol* **74**:965–974.
546 38. **Truett GE, Heeger P, Mynatt RL, Truett AA, Walker JA, Warman ML.** 2000. Preparation of
547 PCR-quality mouse genomic DNA with hot sodium hydroxide and tris (HotSHOT). *BioTechniques*
548 **29**:52, 54.
549 39. **Leib DA, Coen DM, Bogard CL, Hicks KA, Yager DR, Knipe DM, Tyler KL, Schaffer PA.**
550 1989. Immediate-early regulatory gene mutants define different stages in the establishment and
551 reactivation of herpes simplex virus latency. *J Virol* **63**:759–768.
552 40. **Katzenell S, Chen Y, Parker ZM, Leib DA.** 2014. The differential interferon responses of two
553 strains of Stat1-deficient mice do not alter susceptibility to HSV-1 and VSV in vivo. *Virology* **450–451**:350–354.
555 41. **Lizotte PH, Baird JR, Stevens CA, Lauer P, Green WR, Brockstedt DG, Fiering SN.** 2014.
556 Attenuated Listeria monocytogenes reprograms M2-polarized tumor-associated macrophages in
557 ovarian cancer leading to iNOS-mediated tumor cell lysis. *Oncimmunology* **3**:e28926.
558 42. **Livak KJ, Schmittgen TD.** 2001. Analysis of relative gene expression data using real-time
559 quantitative PCR and the 2(-Delta Delta C(T)) Method. *Methods* **25**:402–408.
560 43. **Luker GD, Bardill JP, Prior JL, Pica CM, Piwnica-Worms D, Leib DA.** 2002. Noninvasive
561 Bioluminescence Imaging of Herpes Simplex Virus Type 1 Infection and Therapy in Living Mice. *J
562 Virol* **76**:12149–12161.
563 44. **Pasieka TJ, Collins L, O'Connor MA, Chen Y, Parker ZM, Berwin BL, Piwnica-Worms DR,
564 Leib DA.** 2011. Bioluminescent Imaging Reveals Divergent Viral Pathogenesis in Two Strains of
565 Stat1-Deficient Mice, and in $\alpha\beta\gamma$ Interferon Receptor-Deficient Mice. *PLoS One* **6**.
566 45. **Liu S, Cai X, Wu J, Cong Q, Chen X, Li T, Du F, Ren J, Wu Y-T, Grishin NV, Chen ZJ.** 2015.
567 Phosphorylation of innate immune adaptor proteins MAVS, STING, and TRIF induces IRF3
568 activation. *Science* **347**:aaa2630.
569 46. **Sun L, Wu J, Du F, Chen X, Chen ZJ.** 2013. Cyclic GMP-AMP Synthase Is a Cytosolic DNA
570 Sensor That Activates the Type I Interferon Pathway. *Science* **339**:786–791.
571 47. **Wu J, Sun L, Chen X, Du F, Shi H, Chen C, Chen ZJ.** 2013. Cyclic GMP-AMP Is an Endogenous
572 Second Messenger in Innate Immune Signaling by Cytosolic DNA. *Science* **339**:826–830.
573 48. **Bryant-Hudson KM, Gurung HR, Zheng M, Carr DJJ.** 2014. Tumor Necrosis Factor Alpha and
574 Interleukin-6 Facilitate Corneal Lymphangiogenesis in Response to Herpes Simplex Virus 1
575 Infection. *J Virol* **88**:14451–14457.
576 49. **Li H, Zhang J, Kumar A, Zheng M, Atherton SS, Yu F-SX.** 2006. Herpes simplex virus 1
577 infection induces the expression of proinflammatory cytokines, interferons and TLR7 in human
578 corneal epithelial cells. *Immunology* **117**:167–176.
579 50. **Burdette DL, Vance RE.** 2013. STING and the innate immune response to nucleic acids in the
580 cytosol. *Nature Immunology* **14**:19–26.
581 51. **He B, Gross M, Roizman B.** 1997. The γ 134.5 protein of herpes simplex virus 1 complexes with
582 protein phosphatase 1 α to dephosphorylate the α subunit of the eukaryotic translation initiation
583 factor 2 and preclude the shutoff of protein synthesis by double-stranded RNA-activated
584 protein kinase. *Proc Natl Acad Sci U S A* **94**:843–848.
585 52. **Verpoorten D, Ma Y, Hou S, Yan Z, He B.** 2009. Control of TANK-binding Kinase 1-mediated
586 Signaling by the γ 134.5 Protein of Herpes Simplex Virus 1. *Journal of Biological Chemistry*
587 **284**:1097–1105.
588 53. **Sauer J-D, Sotelo-Troha K, Moltke J von, Monroe KM, Rae CS, Brubaker SW, Hyodo M,
589 Hayakawa Y, Woodward JJ, Portnoy DA, Vance RE.** 2011. The N-ethyl-N-nitrosourea-induced
590 Goldenticket mouse mutant reveals an essential function of Sting in the in vivo interferon response
591 to Listeria monocytogenes and cyclic dinucleotides. *Infect Immun* **79**:688–694.

STING and HSV-1 pathogenesis

- 592 54. **Dey B, Dey RJ, Cheung LS, Pokkali S, Guo H, Lee J-H, Bishai WR.** 2015. A bacterial cyclic
593 dinucleotide activates the cytosolic surveillance pathway and mediates innate resistance to
594 tuberculosis. *Nat Med* **21**:401–406.
595
- 596 55. **Menachery VD, Pasieka TJ, Leib DA.** 2010. Interferon Regulatory Factor 3-Dependent Pathways
597 Are Critical for Control of Herpes Simplex Virus Type 1 Central Nervous System Infection. *J Virol*
598 **84**:9685–9694.
- 599 56. **Honda K, Yanai H, Negishi H, Asagiri M, Sato M, Mizutani T, Shimada N, Ohba Y, Takaoka
600 A, Yoshida N, Taniguchi T.** 2005. IRF-7 is the master regulator of type-I interferon-dependent
601 immune responses. *Nature* **434**:772–777.
- 602 57. **Blaauboer SM, Gabrielle VD, Jin L.** 2013. MPYS/STING-Mediated TNF- α , Not Type I IFN, Is
603 Essential for the Mucosal Adjuvant Activity of (3'-5')-Cyclic-Di-Guanosine-Monophosphate In
604 Vivo. *J Immunol* **130**:1812.
- 605 58. **Yordy B, Iijima N, Huttner A, Leib D, Iwasaki A.** 2012. A Neuron-Specific Role for Autophagy in
606 Antiviral Defense against Herpes Simplex Virus. *Cell Host & Microbe* **12**:334–345.
- 607 59. **Griffin DE.** 2010. Recovery from viral encephalomyelitis: immune-mediated noncytolytic virus
608 clearance from neurons. *Immunol Res* **47**:123–133.
- 609 60. **Liang Q, Seo GJ, Choi YJ, Ge J, Rodgers MA, Shi M, Jung JU.** 2014. Autophagy side of
610 MB21D1/cGAS DNA sensor. *Autophagy* **10**:1146–1147.
- 611 61. **Rasmussen SB, Horan KA, Holm CK, Stranks AJ, Mettenleiter TC, Simon AK, Jensen SB,
612 Rixon FJ, He B, Paludan SR.** 2011. Activation of autophagy by α -herpesviruses in myeloid cells is
613 mediated by cytoplasmic viral DNA through a mechanism dependent on stimulator of IFN genes. *J
614 Immunol* **187**:5268–5276.
- 615 62. **Wu C, Orozco C, Boyer J, Leglise M, Goodale J, Batalov S, Hodge CL, Haase J, Janes J, Huss
616 JW, Su AI.** 2009. BioGPS: an extensible and customizable portal for querying and organizing gene
617 annotation resources. *Genome Biology* **10**:R130.
- 618 63. **Lattin JE, Schroder K, Su AI, Walker JR, Zhang J, Wiltshire T, Saijo K, Glass CK, Hume DA,
619 Kellie S, Sweet MJ.** 2008. Expression analysis of G Protein-Coupled Receptors in mouse
620 macrophages. *Immunome Res* **4**:5.
- 621 64. **Cheng G, Yang K, He B.** 2003. Dephosphorylation of eIF-2alpha mediated by the gamma(1)34.5
622 protein of herpes simplex virus type 1 is required for viral response to interferon but is not sufficient
623 for efficient viral replication. *J Virol* **77**:10154–10161.
- 624 65. **Kalamvoki M, Roizman B.** 2014. HSV-1 degrades, stabilizes, requires, or is stung by STING
625 depending on ICP0, the US3 protein kinase, and cell derivation. *Proc Natl Acad Sci U S A*
626 **111**:E611–E617.
- 627
- 628
- 629

STING and HSV-1 pathogenesis

630 **FIGURE LEGENDS**

631 FIG 1. Survival of STING^{-/-} and littermate control mice following corneal, iv, or ic infection. STING^{-/-} and
632 control mice were infected with 1×10^7 pfu HSV-1 KOS total (A) via the cornea, (B) iv, or (C) with 1×10^4
633 pfu HSV-1 KOS ic. Survival was recorded until endpoint criteria were met. (D) Brain titers of STING^{-/-}
634 and control mice infected with 1×10^4 pfu HSV-1 (KOS) ic and sacrificed on day 3 postinfection.
635 **=p<0.005 Statistical significance was determined by a Mantel-Cox test, with two independent
636 experiments performed with ≥ 9 mice.

637

638 FIG 2. Bioluminescent imaging (BLI) and quantification of HSV-1 (KOSDLux) in STING^{-/-} and littermate
639 control mice following corneal infection. (A) BLI of STING^{-/-} and control mice following corneal
640 infection with 2×10^6 pfu /eye KOSDLux. All images are formatted to a log scale with a minimum 5×10^4
641 p/sec/cm²/sr (purple) and max 1×10^6 p/sec/cm²/sr (red). (B) Quantification of total photon flux performed
642 on heads of all animals imaged using region of interest (ROI) analysis in Living Image software
643 (Xenogen). Data show significant differences between STING^{-/-} and control mice using area under the
644 curve analysis and an unpaired two-tailed t-test ($p=0.0171$). Results are from three independent
645 experiments with ≥ 9 mice.

646

647 FIG 3. Viral titers of STING^{-/-} and littermate control mice following corneal infection with 2×10^6 pfu/eye
648 of HSV-1 (KOS). Mice sacrificed on days 3 and 5 were used to collect titer data for (A) eye swabs, (B)
649 trigeminal ganglia, (C) brain stems, and (D) brains. Periorbital disease (E) and weight change (F) of
650 STING^{-/-} and control mice were measured by a masked observer (20). **=p<0.005, ***=p<0.0005.
651 Statistical significance was tested using an unpaired two-tailed t-test for each day. Disease scores and
652 weights post infection were measured during two independent experiments, using a total of 14 to 23 mice
653 per group.

654

STING and HSV-1 pathogenesis

655 FIG 4. Interferon responses following corneal or intracranial HSV-1 KOS infection. (A) IFN β ELISA of
656 STING $^{-/-}$ and control corneas 3 days following infection with 2x10 6 pfu/eye HSV-1 KOS. (B) IFN β
657 ELISA assays on STING $^{-/-}$ and littermate control brains 3 days following ic infection with 1x10 4 pfu
658 HSV-1 KOS. (C) Real-time PCR of *IFIT1* mRNA expression relative to control mock infected mice
659 normalized to GAPDH, in the corneas of STING $^{-/-}$ and control mice 3 days post corneal infection with
660 2x10 6 pfu/eye HSV-1 KOS. (D) Real-time PCR of *IFIT1* mRNA expression relative to control mock
661 infected mice normalized to GAPDH, in the brains of STING $^{-/-}$ and littermate control mice 3 days post ic
662 infection with 1x10 4 pfu/eye HSV-1 KOS. *= $p<0.05$ Statistical significance was determined using an
663 unpaired two-tailed t-test for IFN β ELISAS and *IFIT1* mRNA expression results. IFN β ELISAs were
664 carried out in two independent experiments on a total number of mice as follows: corneal infection, WT
665 n=7 and STING $^{-/-}$ n=7; ic infection WT n=12 and STING $^{-/-}$ n=14. *IFIT1* real-time PCR was carried out in
666 two independent experiments on a total of 7 mice per group.

667

668 FIG 5. Cytokine RNA expression in infected STING $^{-/-}$ and littermate control mice 3 days postinfection.
669 Real-time PCR of *TNF α* mRNA expression, relative to control mock infected mice performed on (A) the
670 excised corneas of STING $^{-/-}$ and control mice 3 days postinfection with 2x10 6 pfu/eye HSV-1 KOS or (B)
671 excised brains of 3 days post intracranial infection with 1x10 4 pfu HSV-1 KOS. Luminex analysis of
672 CXCL9 in (C) corneas of mice 3 days post corneal infection with 2x10 6 pfu/eye HSV-1 KOS or (D)
673 brains of mice 3 days post intracranial infection with 1x10 4 pfu HSV-1 KOS. *= $p<0.05$ Statistical
674 significance was determined using an unpaired two-tailed t-test for *TNF α* expression and CXCL9
675 concentration results. *TNF α* real-time PCR and CXCL9 was carried out in two independent experiments
676 on a total of \geq 5 mice per group. CXCL9 cytokine quantification was carried out in two independent
677 experiments on a total of 5 mice per group.

678

679 FIG 6. Survival analysis of STING $^{-/-}$ and littermate control mice following intracranial infection with
680 2x10 4 pfu of (A) HSV-1strain 17, (B) Δ BBD, (C) Δ γ 34.5, and (D) Δ TK.. Mortality was recorded upon

STING and HSV-1 pathogenesis

681 endpoint criteria being met. Statistical significance was determined by a Mantel-Cox test. For each type
682 of infection two independent experiments were performed. The number of mice used for each survival
683 experiment are as follows: strain 17, WT n= 6, STING^{-/-} n=10; ΔBBB, WT n=6, STING^{-/-} n=7; Δγ34.5,
684 WT n=9, STING^{-/-} n=10; ΔTK, WT n=11, STING^{-/-} n=8.

685

686 FIG 7. Survival analysis of STING^{-/-} and littermate control mice following corneal infection with 1x10⁵
687 pfu/eye of (A) HSV-1 strain 17, (B) ΔBBB, (C) Δγ34.5, and (D) ΔTK. Mortality was recorded upon
688 endpoint criteria being met. Statistical significance was determined by a Mantel-Cox test. For each
689 infection two independent experiments were performed. The number of mice used for each survival
690 experiment are as follows: strain 17, WT n=7, STING^{-/-} n=7; ΔBBB, WT n=6, STING^{-/-} n=6; Δγ34.5, WT
691 n=5, STING^{-/-} n=6; ΔTK, WT n=4, STING^{-/-} n=5.

692

Figure 1

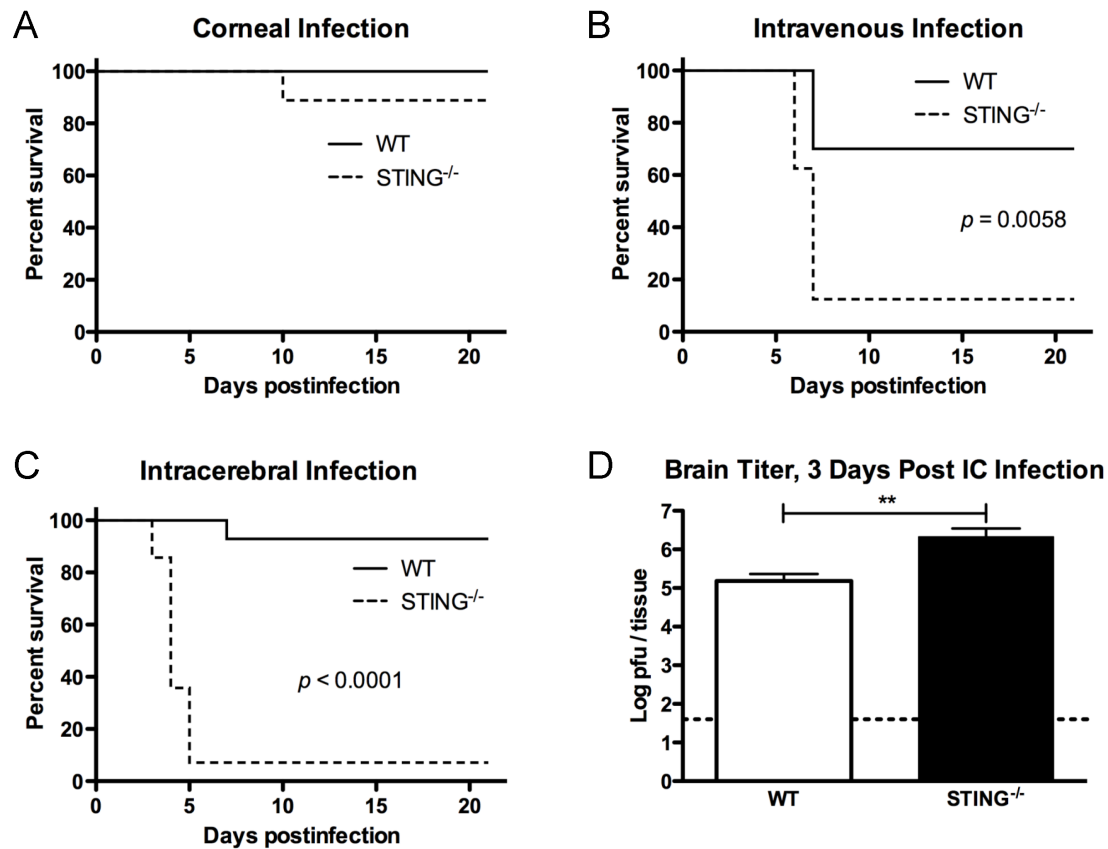


Figure 2

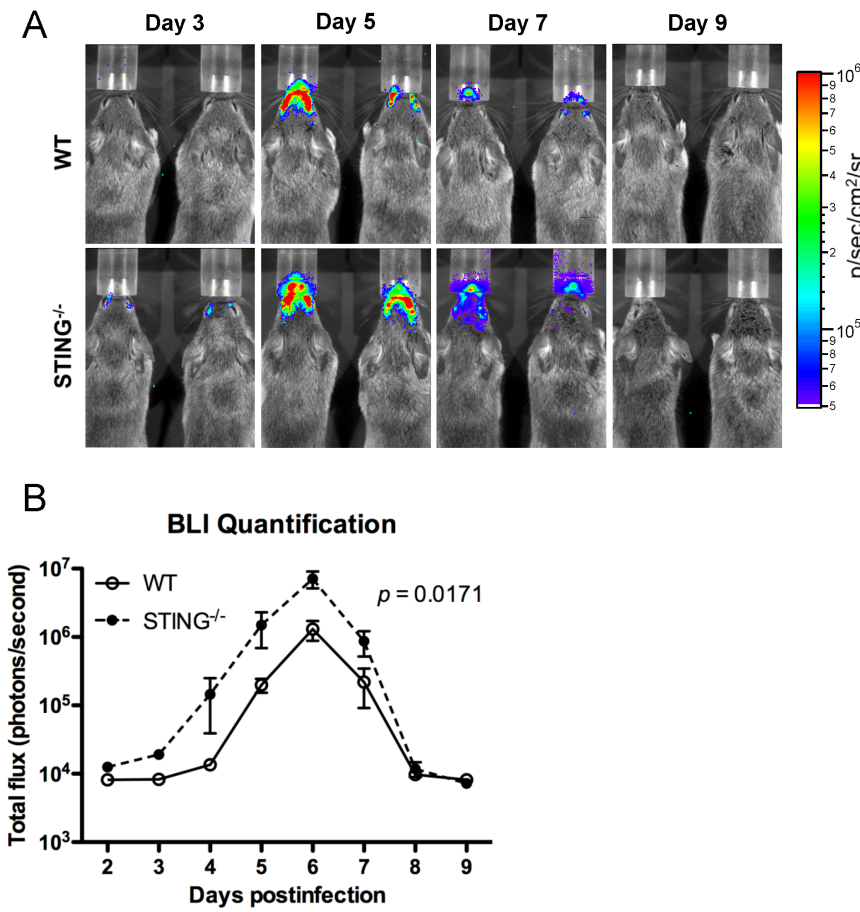


Figure 3

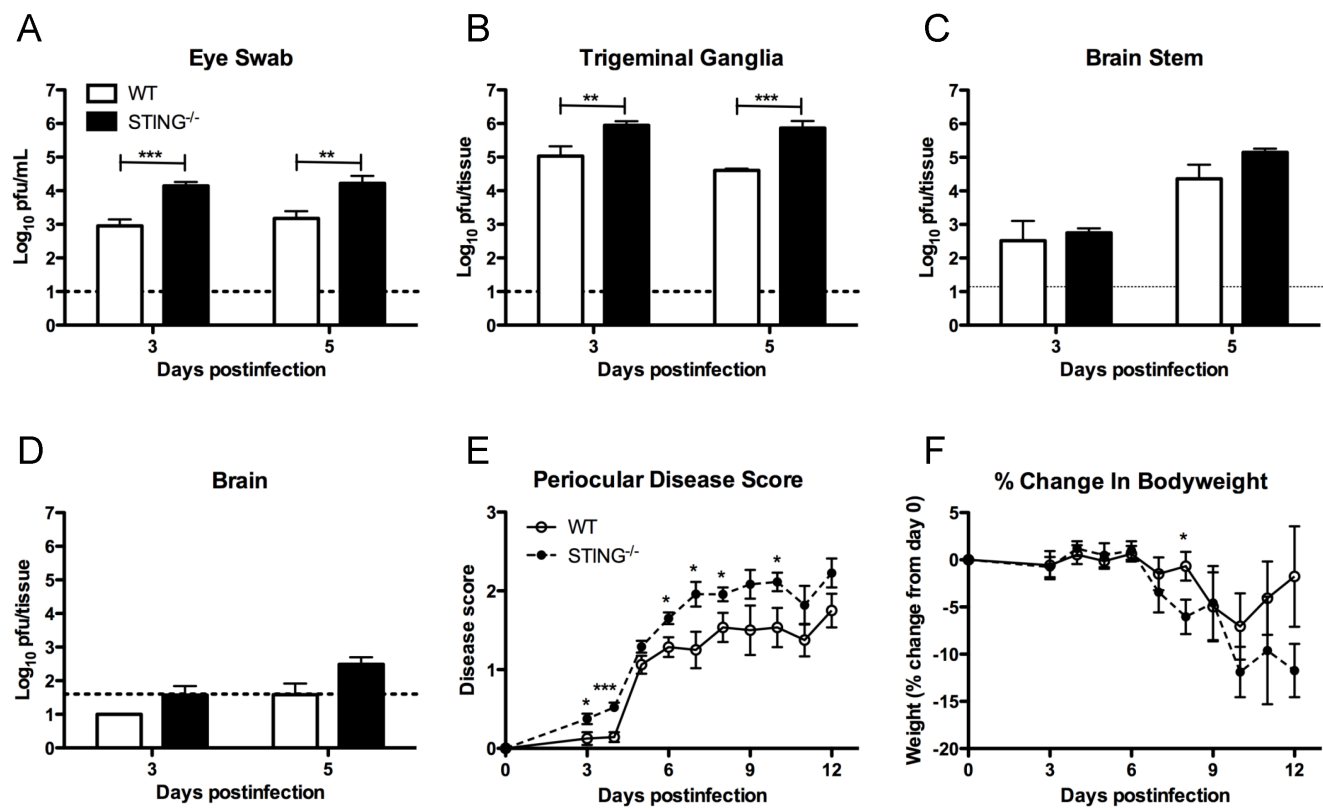


Figure 4

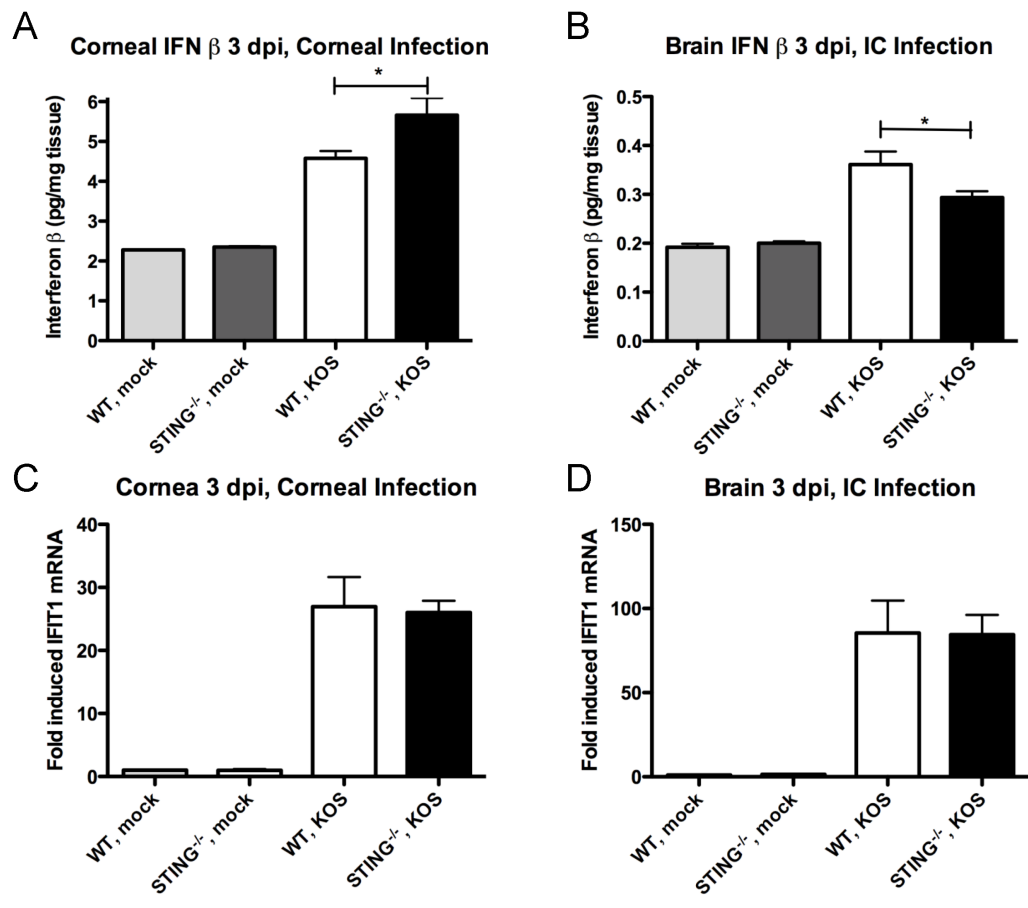


Figure 5

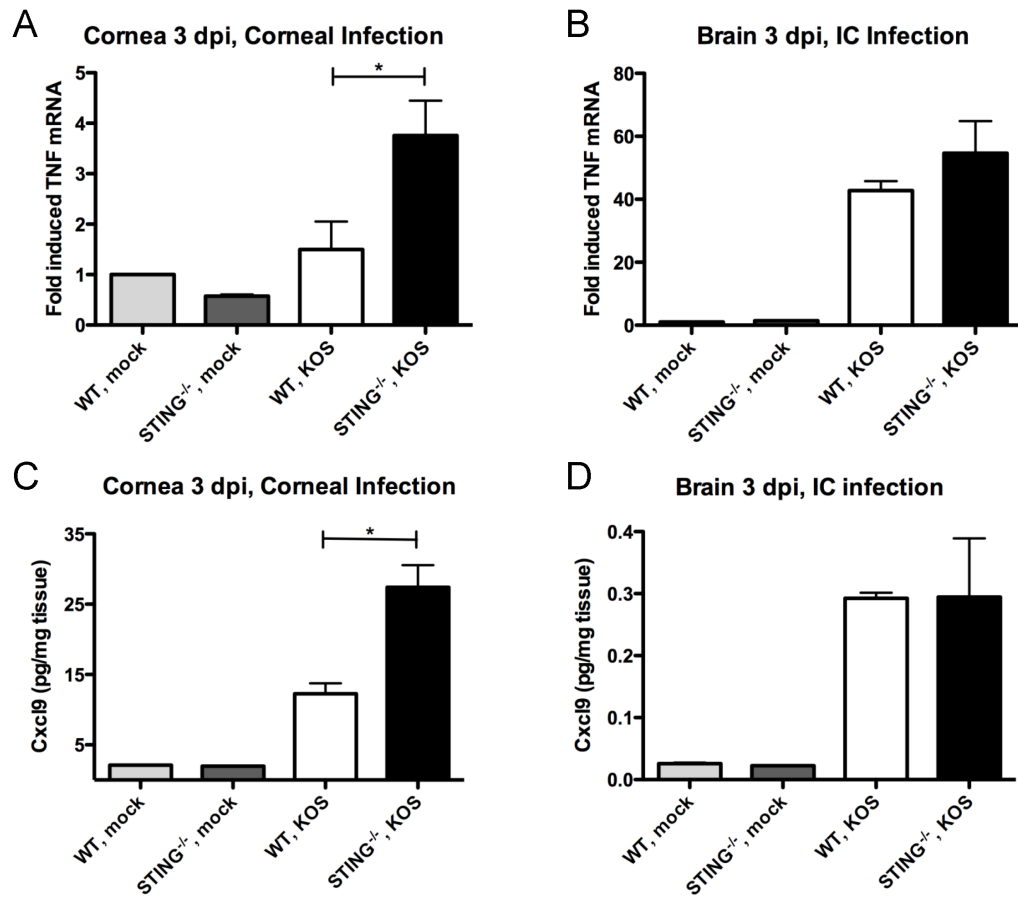


Figure 6

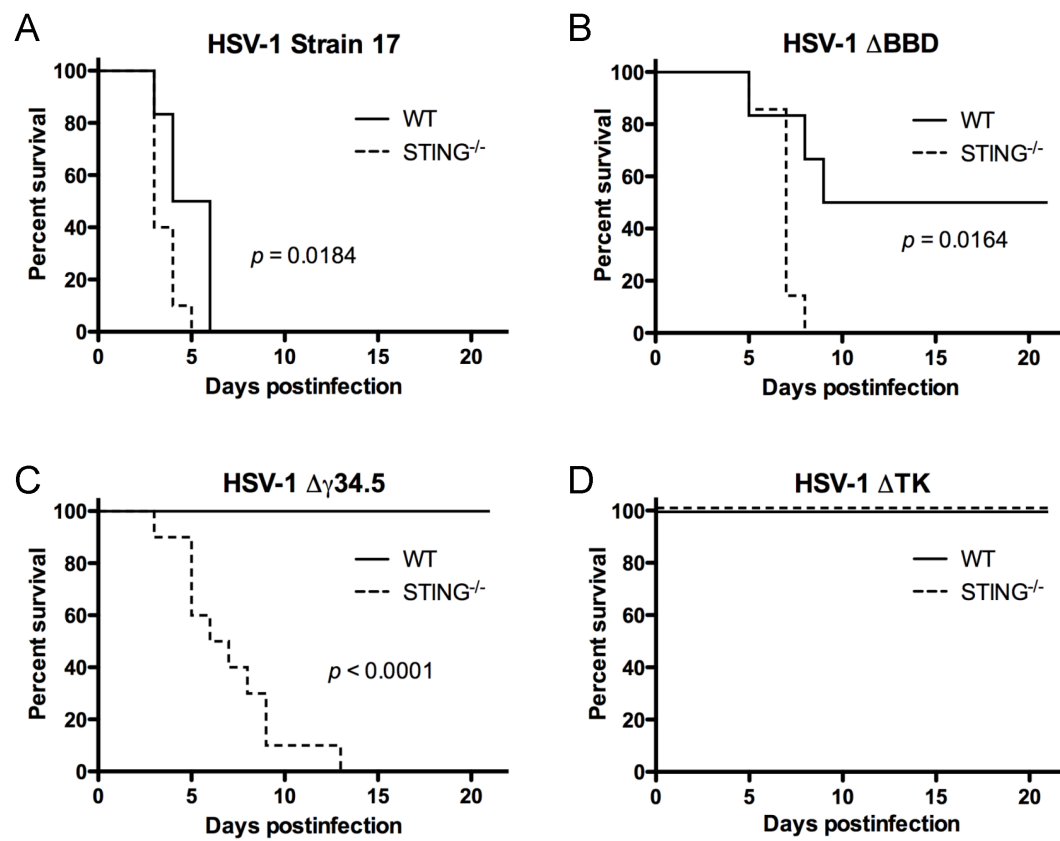


Figure 7

